

## ORIGINAL ARTICLE

## L-carnitine enhances axonal plasticity and improves white-matter lesions after chronic hypoperfusion in rat brain

Yuji Ueno<sup>1,2</sup>, Masato Koike<sup>3</sup>, Yoshiaki Shimada<sup>2</sup>, Hideki Shimura<sup>1</sup>, Kenichiro Hira<sup>2</sup>, Ryota Tanaka<sup>2</sup>, Yasuo Uchiyama<sup>3,4</sup>, Nobutaka Hattori<sup>2</sup> and Takao Urabe<sup>1</sup>

Chronic cerebral hypoperfusion causes white-matter lesions (WMLs) with oxidative stress and cognitive impairment. However, the biologic mechanisms that regulate axonal plasticity under chronic cerebral hypoperfusion have not been fully investigated. Here, we investigated whether L-carnitine, an antioxidant agent, enhances axonal plasticity and oligodendrocyte expression, and explored the signaling pathways that mediate axonal plasticity in a rat chronic hypoperfusion model. Adult male Wistar rats subjected to ligation of the bilateral common carotid arteries (LBCCA) were treated with or without L-carnitine. L-carnitine-treated rats exhibited significantly reduced escape latency in the Morris water maze task at 28 days after chronic hypoperfusion. Western blot analysis indicated that L-carnitine increased levels of phosphorylated high-molecular weight neurofilament (pNFH), concurrent with a reduction in phosphorylated phosphatase tensin homolog deleted on chromosome 10 (PTEN), and increased phosphorylated Akt and mammalian target of rapamycin (mTOR) at 28 days after chronic hypoperfusion. L-carnitine reduced lipid peroxidation and oxidative DNA damage, and enhanced oligodendrocyte marker expression and myelin sheath thickness after chronic hypoperfusion. L-carnitine regulates the PTEN/Akt/mTOR signaling pathway, and enhances axonal plasticity while concurrently ameliorating oxidative stress and increasing oligodendrocyte myelination of axons, thereby improving WMLs and cognitive impairment in a rat chronic hypoperfusion model.

*Journal of Cerebral Blood Flow & Metabolism* (2015) **35**, 382–391; doi:10.1038/jcbfm.2014.210; published online 3 December 2014

**Keywords:** axonal outgrowth; chronic hypoperfusion; L-carnitine; oxidative stress; stroke

## INTRODUCTION

Cerebral white matter constitutes 50% of human brain mass and contains abundant axons and oligodendrocytes.<sup>1</sup> Cerebral white matter is damaged by a variety of neurologic disorders including ischemic stroke, and white-matter lesions (WMLs) have been associated with cognitive impairment.<sup>2</sup> Oligodendrocytes are lipid rich and exhibit low levels of antioxidant enzymes, which reduce their ability to cope with the increased generation of reactive oxygen species during ischemic insults.<sup>3</sup> Axons are vulnerable to ischemia, and are also damaged by axon–oligodendrocyte interactions after ischemia.<sup>4</sup> Permanent occlusion of both common carotid arteries can induce chronic cerebral hypoperfusion in experimental animals, which results in WMLs in the corpus callosum.<sup>5–7</sup> Various pathogenic factors are implicated in WMLs, including oxidative stress, inflammatory reactions, and endothelial injuries.<sup>6</sup>

L-carnitine therapy is required for children with an inborn error of metabolism as well as chronic debilitating diseases including cancer, diabetes mellitus, and chronic kidney disease.<sup>8,9</sup> In such chronic diseases, L-carnitine has a pivotal role in suppressing inflammatory reactions, oxidative stress, and apoptosis.<sup>9</sup> L-carnitine

has also been proven beneficial in ischemic heart disease and peripheral artery disease.<sup>10,11</sup> Continuous supplementation with L-carnitine increases carnitine content, stimulates pyruvate oxidation, and thereby remodels the myocardium and improves cardiac dysfunction.<sup>12</sup> However, little information is available on the effect of L-carnitine on cerebral ischemia.<sup>13–15</sup> To date, the effect of L-carnitine on WMLs induced by chronic cerebral hypoperfusion is essentially unknown.

Axonal outgrowth and plasticity are critical processes during brain repair after stroke injury, and related to improvements in neurologic deficits after stroke.<sup>16,17</sup> Stroke induces axonal outgrowth, and emerging data indicate that the phosphoinositide 3-kinase/Akt/glycogen synthase kinase-3 $\beta$  signaling pathway enhances axonal outgrowth after stroke.<sup>18</sup> To date, the mechanisms that regulate axonal plasticity after chronic hypoperfusion have not been extensively studied. In the present study, we used a rat chronic hypoperfusion model to determine whether L-carnitine exerts a neuroprotective role in WMLs and enhances axonal plasticity, and investigated the signaling pathways that mediate axonal plasticity.

<sup>1</sup>Department of Neurology, Juntendo University Urayasu Hospital, Chiba, Japan; <sup>2</sup>Department of Neurology, Juntendo University School of Medicine, Tokyo, Japan; <sup>3</sup>Department of Cell Biology and Neuroscience, Juntendo University School of Medicine, Tokyo, Japan and <sup>4</sup>Department of Cellular and Molecular Neuropathology, Juntendo University Graduate School of Medicine, Tokyo, Japan. Correspondence: Dr Y Ueno, Department of Neurology, Juntendo University School of Medicine, 2-1-1 Hongo, Bunkyo, Tokyo 113-8421, Japan.

E-mail: yuji-u@juntendo.ac.jp

This study was supported in part by a High Technology Research Center grant and a grant-in-aid for exploratory research from the Ministry of Education, Culture, Sports, Science, and Technology, Japan. This study was also supported in part by a Grant-in-Aid (S1311011) from the Foundation for Strategic Research Projects in Private Universities from MEXT. This study was also supported in part by the Comprehensive Brain Science Network (CBSN).

Received 30 August 2014; revised 28 October 2014; accepted 30 October 2014; published online 3 December 2014

## MATERIALS AND METHODS

### Chronic Cerebral Hypoperfusion

All animals used in the present study were acquired and cared for in accordance with the guidelines published in the National Institutes of Health Guide for the Care and Use of Laboratory Animals. The Animal Care Committee of Juntendo University approved all animal protocols used in the present study, and efforts were made to minimize the number of animals used and their suffering. Adult male Wistar rats (9 to 11 weeks old) weighing 280 to 320 g were purchased from Charles River Institute (Kanagawa, Japan). Chronic cerebral hypoperfusion was induced by ligation of both common carotid arteries (LBCCA), as described previously.<sup>4–6</sup> Rats were anesthetized with 1.0% to 2.0% isoflurane in 30% O<sub>2</sub> and 70% N<sub>2</sub>O. Through a midline incision, the bilateral common carotid arteries were carefully separated from the cervical sympathetic and vagal nerves, and ligatured permanently. During this procedure, the body temperature was maintained at 37.0 ± 0.5°C. Rats at baseline (before LBCCA) or 7, 14, 21, and 28 days after LBCCA were reanesthetized with 1% isoflurane, 70% N<sub>2</sub>O:30% O<sub>2</sub>, and transcardially perfused with phosphate-buffered saline (PBS) followed by 4% paraformaldehyde. The brain was dissected out immediately, postfixed in 4% paraformaldehyde for 48 hours, and stored in 30% sucrose in 0.1 mol/L PBS. For immunohistochemistry, 20- $\mu$ m-thick free-floating coronal sections of rat brain were prepared for staining.

### Drug Administration and Classification

Rats were randomly divided into the following groups: (1) L-carnitine group: post-LBCCA, rats were treated *per os* daily with 600 mg/kg (in 0.7 mL saline) L-carnitine (Sigma Aldrich, Inc., St Louis, MO, USA) using an oral gavage tube, until euthanasia;<sup>19</sup> (2) vehicle group: rats received *per os* administration of saline, volumes similar to the L-carnitine group, using a gavage tube; and (3) control sham-operated group: rats underwent the protocol described for the vehicle group, but were spared LBCCA.

### Measurement of Cerebral Blood Flow

Cerebral blood flow (CBF) was measured at a left temporal window, using laser Doppler flowmetry (Laser Tissue Blood Flow Meter FLO-C1; Omega Wave, Inc., Tokyo, Japan). A flat rectangular sheet-shaped probe (7.5 mm in length and 1.0 mm in depth) was positioned between the temporal muscle and the lateral aspect of the skull, according to a previously published method.<sup>20</sup> Craniotomy was not required and CBF was monitored continuously in 3 to 5 minutes sessions before, immediately after, and 7, 14, 21, and 28 days after LBCCA. Reproducibly recorded CBF velocities were obtained.

### Water Maze Task

The water maze task was performed to evaluate deficits in learning and spatial memory induced by cerebral chronic hypoperfusion, using the method described previously.<sup>6</sup> A circular transparent acrylic platform with a radius of 20 cm was placed in a 150-cm diameter circular pool filled with water (20 cm depth) set at 22 ± 1°C, with the top surface of the platform positioned 3 cm below the surface of the water. The water in the pool was made opaque with milk so that the rats were unable to see the underwater platform. Rats were released facing a wall from a standard point, and the time taken to escape to the platform was recorded as the escape latency. The rats performed five trials per day, with a constant intertrial interval of 30 minutes, for 3 consecutive days before LBCCA. The escape latency was analyzed before LBCCA and 7, 14, 21, and 28 days after LBCCA.

### Rotarod Performance Test

The rotarod performance test was performed to assess motor dysfunction induced by chronic cerebral hypoperfusion. After 3 consecutive days of training before the operation, rotarod performance was evaluated at 7, 14, 21, and 28 days after LBCCA. The speed was slowly increased from 10 to 40 r.p.m. (0.005 to 0.08 g) over a period of 4 minutes. The trial ended when the animal falls off the rungs. The maximum duration on the device was recorded with three rotarod measurements. Rotarod test data are presented as percentages of the maximal duration, compared with the internal baseline control.

### Immunohistochemistry and Double Immunofluorescence

Immunohistochemistry was performed on brain sections, as previously described.<sup>18</sup> After incubation in 0.3% H<sub>2</sub>O<sub>2</sub> followed by 10% block ace in 0.1 mol/L PBS, coronal sections of the corpus callosum were immunostained overnight at 4°C using a mouse monoclonal antibody against 4-

hydroxy-2-nonenal (HNE, a marker of lipid peroxidation; dilution, 40:1; Japan Institute for the Control of Aging, Japan), a mouse monoclonal antibody against 8-hydroxy-deoxyguanosine (8OHdG, a marker of oxidative DNA damage; dilution 100:1; Japan Institute for the Control of Aging), a rabbit polyclonal antibody against glutathione-S-transferase-pi (GST-pi, a marker of oligodendrocytes; dilution, 1,000:1; Chemicon International, Inc., Temecula, CA, USA), and ss-DNA (a marker of apoptotic cells; dilution, 100:1; Dako Corporation, Carpinteria, CA, USA) staining. The sections were then treated with secondary antibodies (dilution, 300:1; Vectastain; Vector Laboratories, Burlingame, CA, USA). Immunoreactivity was subsequently visualized using the avidin-biotin complex method (Vectastain, Vector Laboratories) and developed with diaminobenzidine. For double immunofluorescence staining, mouse anti-SMI31 (a marker of phosphorylated high molecular weight neurofilament, pNFH; 1:100; Covance, Emeryville, CA, USA), mouse anti-SMI32 (a marker of nonphosphorylated NFH, 1:100; Covance), and rat anti-myelin basic protein (MBP; 1:100; Millipore, Philadelphia, PA, USA) were used. After washing with PBS three times, rat coronal sections were incubated overnight at 4°C with the primary antibodies listed above, and subsequently with Cy3 or FITC-conjugated secondary antibodies for 2 hours at room temperature.

### Electron Microscopy

Anesthetized rats were fixed by cardiac perfusion with 2% paraformaldehyde/2% glutaraldehyde buffered with 0.1 mol/L phosphate buffer. Brain tissues were quickly excised and subsequently immersed in the same fixative overnight at 4°C. Using Rodent Brain Matrices (ASI Instruments, Warren, MI, USA) 1-mm-thick brain slices were made. The samples were postfixed with 2% OsO<sub>4</sub> in 0.1 mol/L phosphate buffer for 2 hours at 4°C in the dark, block-stained in 1% uranyl acetate for 1 hour, dehydrated with a graded series of aqueous alcohol solutions, and embedded in Epon 812 (TAAB, Barks, UK). Silver sections were cut with an ultramicrotome (Leica UC6; Leica Microsystems, Vienna, Austria), stained with uranyl acetate and lead citrate, and observed with an electron microscope (HT7700; Hitachi, Tokyo, Japan).

### Western Blot

All procedures were performed at 4°C. To prepare samples for western blot, corpus callosum tissues were extracted from rat brains, and transferred into 700  $\mu$ L homogenization buffer (0.25 mol/L sucrose, 0.15 mol/L KCl, 10 mmol/L Tris-Cl, pH 7.5, 1 mmol/L EDTA, 0.5% fatty acid-free BSA) containing Protease Inhibitor (Calbiochem, San Diego, CA, USA), and homogenized with 3 × 10 strokes using a Dounce tissue grinder (Wheaton Scientific, Millville, NJ, USA). The homogenates were centrifuged 10 minutes at 700 g. The supernatant was collected and filtered through layers of cheesecloth and centrifuged 15 minutes at 12,000 g. The final supernatant was referred to as cytosol and used for western blotting.<sup>21</sup> Western blots were performed according to published methods.<sup>6</sup> Briefly, equal amounts of total protein for each sample were loaded on 10% SDS-polyacrylamide gels. After electrophoresis, the proteins were transferred onto nitrocellulose membranes, and the blots were subsequently probed with the following primary antibodies: mouse anti-SMI 31 (1:2,000; Covance), rabbit anti-phosphorylated Akt (Ser 473, 1:1,000; Cell Signaling Technology, Danvers, MA, USA), rabbit anti-Akt (1:2,000; Cell Signaling Technology), rabbit anti-phosphorylated phosphatase and tensin homolog deleted on chromosome 10 (PTEN, Ser 380/Thr 382/383, 1:1,000; Cell Signaling Technology), rabbit anti-PTEN (1:2,000; Cell Signaling Technology), rabbit anti-phosphorylated mammalian target of rapamycin (mTOR, Ser 2448, 1:1,000; Cell Signaling Technology), rabbit anti-mTOR (1:1,000; Cell Signaling Technology), rat anti-MBP (1:2,000; Millipore), rabbit anti-carnitine palmitoyltransferase 1A (CPT1A, 1:1,000; Millipore) and CPT2 (1:1,000; Millipore), and mouse monoclonal anti- $\beta$ -actin (1:10,000; Abcam, Cambridge, MA, USA). Protein levels of PTEN, Akt, mTOR, and  $\beta$ -actin were used as internal controls. Western blots were performed from at least three individual experiments.

### Image Acquisition and Quantification

For histologic experiments, the number of stained cells and the density of axons were analyzed in three coronal sections at 200  $\mu$ m intervals in each rat brain. Two images in the corpus callosum per section were acquired, and ss-DNA-positive cells were counted in the entire area of the corpus callosum. A confocal microscope (LEICA TCS SP5 II, Leica Microsystems) with a 40× objective was used to acquire the images. Images were analyzed using the National Institutes of Health Image analysis program version 1.43, as described previously.<sup>17</sup> Briefly, the pNFH<sup>+</sup>-MBP<sup>+</sup> areas were

split into green and red channels, and images showing common positive areas in both channels were obtained. The intensity levels were then digitally adjusted with pixel intensity thresholds (black pixels represent pNFH<sup>+</sup>-MBP<sup>+</sup> immunoreactive areas). The total area of black pixels was divided by the total area in each image to estimate the degree of axonal plasticity and myelination after LBCCA. Electron microscopy image analysis involved estimating the number of myelinated axons in the corpus callosum. Only myelinated axon profiles with diameters greater than 0.5  $\mu\text{m}$  were included in the counts.<sup>22</sup> Thirty to forty axons were randomly counted in predefined bilateral areas of the corpus callosum in each rat brain. All *in vivo* experiments and measurements were performed in a blinded and randomized manner.

### Statistical Analysis

Values presented in this study are expressed as mean  $\pm$  standard error. All statistical analyses were performed using the Statistical Package for the Social Sciences (version 15; SPSS Inc., Chicago, IL, USA). Student's *t*-test and one-way ANOVA with Bonferroni *post hoc* tests were used when comparing two groups and greater than two groups, respectively. Chi-square tests were used for comparisons of the number of axons according to the axonal diameter among groups. A probability value of  $< 0.05$  was considered as significant.

## RESULTS

### Temporal Changes in Cerebral Blood Flow after Ligation of Both Common Carotid Arteries

Figure 1A shows the temporal changes in CBF in each group. After LBCCA, CBF gradually increased in the vehicle- and L-carnitine-treated rats up to 28 days after LBCCA. There were no significant differences in CBF between the vehicle and L-carnitine-treated rats.

### Effects of L-Carnitine on Learning Memory and Motor Function

Before LBCCA, the majority of the rats escaped within 10 seconds after training in the Morris water maze task. The escape latencies of the sham-operated group were within 10 seconds up to 28 days after LBCCA. The escape latency of the vehicle group gradually increased from 7 to 28 days after LBCCA. At 21 and 28 days after LBCCA, the escape latency of the vehicle group significantly increased compared with the sham-operated group ( $P < 0.01$ , Figure 1B). The L-carnitine-treated rats exhibited shorter latencies than the vehicle-treated group. In particular, at 21 and 28 days after LBCCA the escape latency was significantly different between the vehicle and L-carnitine groups ( $P < 0.05$ , Figure 1B). In the rotarod test, the step out latency did not change after LBCCA, and there were no significant differences among the sham-operated, vehicle-treated, and L-carnitine-treated rats at each time point (Figure 1C). These data suggest that L-carnitine improves cognitive dysfunction induced by chronic cerebral hypoperfusion in the Morris water maze task, while motor function in the rotarod test was not impaired after chronic cerebral hypoperfusion.

### L-carnitine Sustained Cell Viability in Corpus Callosum

The ss-DNA staining experiments indicated that ss-DNA<sup>+</sup> cells were substantially increased from 7 to 28 days after LBCCA from baseline. However, L-carnitine significantly reduced the number of ss-DNA<sup>+</sup> cells at each time point after LBCCA compared with the vehicle group ( $P < 0.05$ , Figures 1D and 1E).

### L-carnitine Enhances Axonal Plasticity after Chronic Hypoperfusion

The pNFH is an abundant architectural cytoskeletal element in axons, participates in axonal growth, and regulates synaptic function.<sup>23,24</sup> On western blot analysis, pNFH density decreased at 14 and 28 days after LBCCA in the vehicle-treated rats. However, L-carnitine significantly increased the density of pNFH compared with the vehicle-treated rats at 28 days after LBCCA ( $P < 0.05$ ,

Figures 2A and 2B). A significant decrease in phosphorylated phosphatase and PTEN at 28 days after LBCCA was observed in L-carnitine-treated rats compared with vehicle-treated rats ( $P < 0.05$ , Figure 3A), together with an elevation of phosphorylated Akt and phosphorylated mTOR ( $P < 0.05$ , Figures 3B and 3C). Our data suggest that L-carnitine enhances pNFH expression related to regulation of the PTEN/Akt/mTOR pathway after chronic cerebral hypoperfusion.

### L-carnitine Reduces Lipid Peroxidation and Oxidative DNA Damage in Oligodendrocytes

MBP is a marker of mature oligodendrocytes. Our data show that MBP levels gradually decreased in vehicle-treated rats and increase in L-carnitine-treated rats from baseline after LBCCA. At 28 days after LBCCA, L-carnitine significantly increases MBP levels compared with vehicle-treated rats ( $P < 0.05$ , Figures 2A and 2C). The number of oligodendrocytes in vehicle-treated rats significantly decreased from baseline at 28 days after LBCCA, while the number of oligodendrocytes in L-carnitine-treated rats was not substantially altered ( $P < 0.05$ , Figures 2D and 2E). To examine oxidative stress in WMLs after LBCCA, lipid peroxidation and oxidative DNA damage were assessed using HNE and 8OHdG staining, respectively. In the vehicle-treated group, HNE<sup>+</sup> cells gradually but substantially increased at 7, 14, 21, and 28 days after LBCCA compared with the sham-operated group ( $P < 0.001$ , Figures 4A and 4B). In the L-carnitine-treated group, HNE<sup>+</sup> cells also increased at each time point after LBCCA. However, HNE<sup>+</sup> cells were significantly decreased at 7, 14, 21, and 28 days after LBCCA compared with the vehicle-treated group ( $P < 0.05$ , Figures 4A and 4B). In the vehicle-treated group, 8OHdG<sup>+</sup> cells were substantially increased at 7, 14, 21, and 28 days compared with the sham-operated group ( $P < 0.001$ , Figures 4C and 4D). L-carnitine significantly reduced the number of 8OHdG<sup>+</sup> cells compared with the vehicle-treated group, and there were no significant differences in the number of 8OHdG<sup>+</sup> cells between the sham-operated group and the L-carnitine-treated group ( $P < 0.01$ , Figures 4C and 4D). Previously, we showed that HNE<sup>+</sup> and 8OHdG<sup>+</sup> cells in the corpus callosum were colocalized with GST-pi<sup>+</sup> cells, a marker of oligodendrocytes.<sup>6</sup> In the current study, HNE<sup>+</sup> cells were colocalized to GST-pi<sup>+</sup> oligodendrocytes (Figure 4E) after LBCCA.

### L-carnitine Enhances Myelin Sheath Growth and Facilitates Myelination of Axons

To examine alterations in axon-oligodendrocyte interactions after LBCCA, we measured the diameter of myelin sheaths using double immunofluorescence staining. The diameter of MBP<sup>+</sup> oligodendrocyte processes decreased at 28 days after LBCCA in vehicle-treated rats from baseline levels ( $P < 0.05$ , Figure 5A). However, L-carnitine substantially increased the diameter of MBP<sup>+</sup> myelin sheaths compared with vehicle-treated rats at 28 days ( $P < 0.001$ , Figure 5A). To analyze myelin sheath thickness in more detail, we used electron microscopy. After LBCCA, myelin sheath thickness in vehicle-treated rats gradually decreased over time from baseline levels (Figure 5B). However, L-carnitine-treated rats exhibited substantially increased myelin sheath thickness after LBCCA (Figure 5B). Myelin sheaths in L-carnitine-treated rats were significantly thicker than those in sham-operated and vehicle-treated rats at 28 days after LBCCA ( $P < 0.001$ , Figure 5C). Concurrently, pNFH<sup>+</sup> axons were well myelinated by MBP<sup>+</sup> oligodendrocytes in the corpus callosum of L-carnitine-treated rats ( $P < 0.05$ , Figure 5D). Thus, axonal damage and oxidative damage in oligodendrocytes were induced after chronic cerebral hypoperfusion. The aforementioned data suggest that continuous treatment with L-carnitine suppresses oxidative stress in oligodendrocytes after LBCCA, and enhances oligodendrocyte marker expression as well as axonal plasticity, thereby facilitating myelination of axons in the chronic stage of chronic cerebral hypoperfusion.

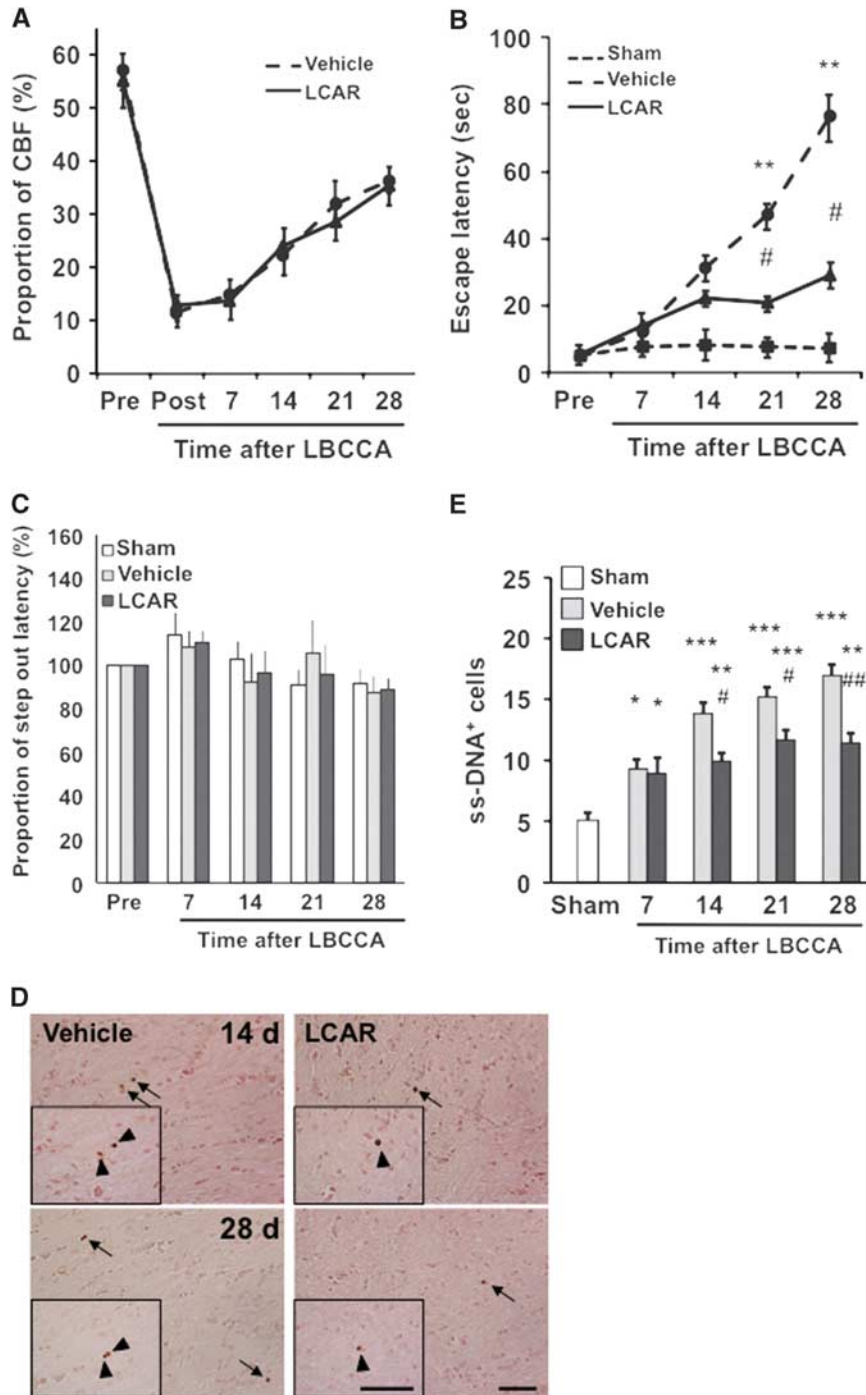


**Figure 1.** Effects of L-carnitine on physiologic parameters and cell viability. **(A)** Temporal changes in cerebral blood flow (CBF) immediately before (pre) and after (post) ligation of bilateral common carotid arteries (LBCCA), as well as postligation (7 to 28 days).  $N = 5/\text{group}$ . **(B)** Morris water maze escape latency pre- and post-LBCCA (7 to 28 days). Values are normalized to the pre-LBCCA latency.  $N = 5/\text{group}$ . **(C)** Rotarod behavioral test performance pre- and post-LBCCA (7 to 28 days). Values are normalized to the pre-LBCCA latency.  $N = 5/\text{group}$ . **(D)** Representative images of ss-DNA immunostaining counterstained with eosin indicating apoptotic cells (arrows, arrowheads in magnified images) in the corpus callosum of vehicle-treated and L-carnitine (LCAR)-treated rats at 14 and 28 days after LBCCA. Bars =  $50\ \mu\text{m}$  and  $20\ \mu\text{m}$  in the larger and inset panels, respectively. **(E)** Quantitation of ss-DNA<sup>+</sup> apoptotic cells in the corpus callosum.  $N = 4/\text{group}$ . Values are expressed as mean  $\pm$  s.e. \* $P < 0.05$ , \*\* $P < 0.01$ , \*\*\* $P < 0.001$  versus the sham-operated group, and # $P < 0.05$  and ## $P < 0.01$  versus the vehicle-treated group.

#### Improvement of Carnitine Homeostasis

To examine mitochondrial membrane transport function, CPT1A and CPT2, inner and outer mitochondrial membrane transporter enzymes, were analyzed using western blots. After LBCCA, protein

levels of CPT1A and CPT2 decreased in vehicle-treated rats. L-carnitine significantly increased CPT1A and CPT2 levels at 28 days after LBCCA compared with vehicle-treated rats, indicating that L-carnitine improves impairment of mitochondrial membrane function induced by chronic cerebral hypoperfusion

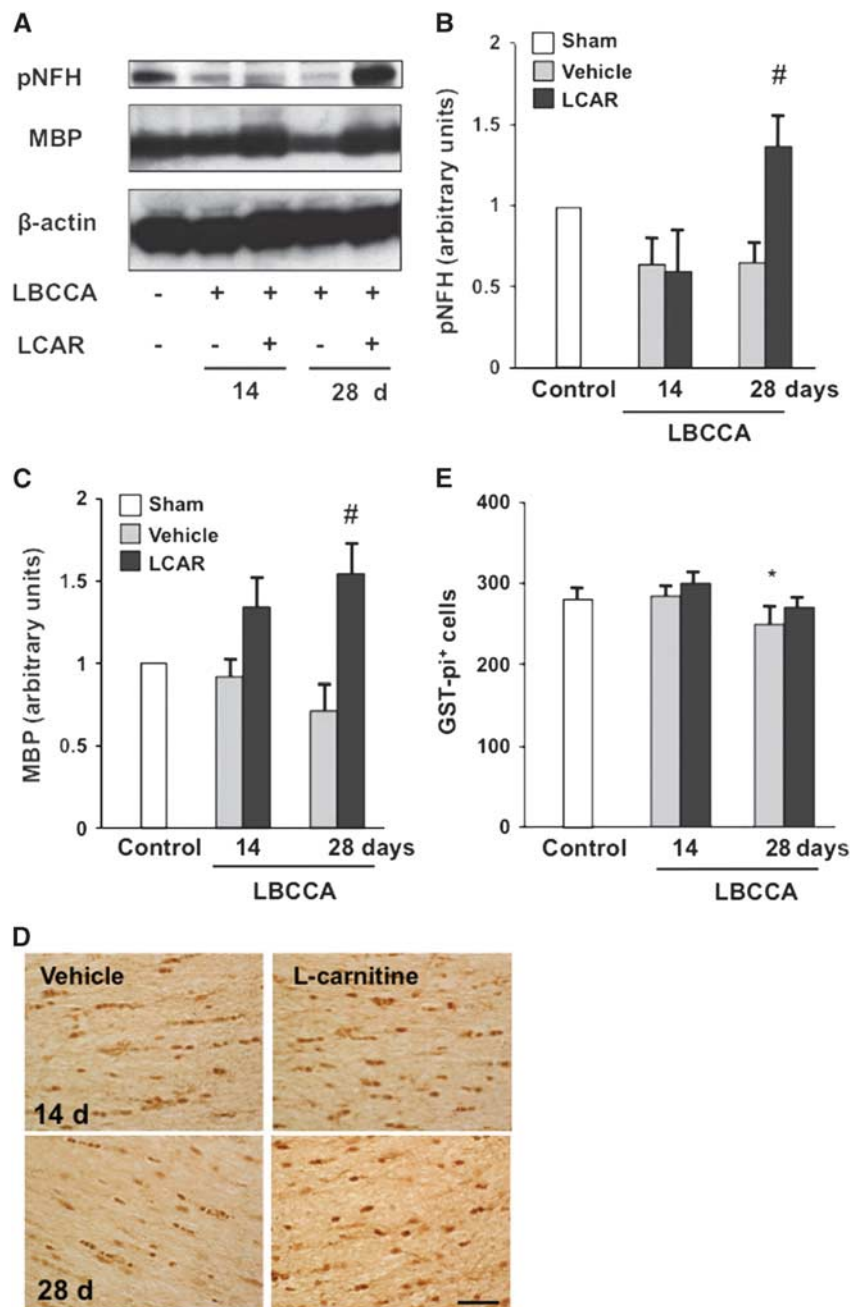


**Figure 2.** L-carnitine increases phosphorylated high molecular weight neurofilament (pNFH) and myelin basic protein (MBP) after chronic hypoperfusion. **(A–C)** pNFH and MBP levels were measured using western blots.  $\beta$ -Actin was used as an internal control.  $N=5$ /group. Values are expressed as mean  $\pm$  s.e.  $^{\#}P < 0.05$  versus the vehicle-treated rats. **(D)** Representative images of glutathione-S-transferase-pi (GST-pi) immunostaining show the mature oligodendrocytes at 14 and 28 days post ligation of the bilateral common carotid (LBCCA) in vehicle-treated and L-carnitine (LCAR)-treated rats. Bars = 50  $\mu$ m. **(E)** Quantitation of GST-pi<sup>+</sup> cell numbers in the corpus callosum.  $N=4$ /group. Values are expressed as mean  $\pm$  s.e.  $^*P < 0.05$  versus the sham-operated group.

( $P < 0.05$ , Figures 6A–6C). Thus, it is suggested that improved mitochondrial membrane function may be associated with increased axonal plasticity and myelination after L-carnitine treatment after LBCCA.

## DISCUSSION

To the best of our knowledge, this is the first study to examine the effect of L-carnitine against WMLs under chronic hypoperfusion. The principal findings presented here were that, in a rat cerebral

chronic hypoperfusion model, L-carnitine: enhanced pNFH levels related to the regulation of the PTEN/Akt/mTOR pathway; suppressed lipid peroxidation products and oxidative DNA damage; sustained cell viability; stimulated myelin sheath growth; facilitated myelination of pNFH<sup>+</sup> axons; improved mitochondrial membrane function in the corpus callosum; and improved spatial learning and memory.

Although CBF measured by laser Doppler flowmetry does not directly represent tissue flow in white matter, development of WMLs is linked to alterations in CBF.<sup>5–7</sup> In the acute phase,

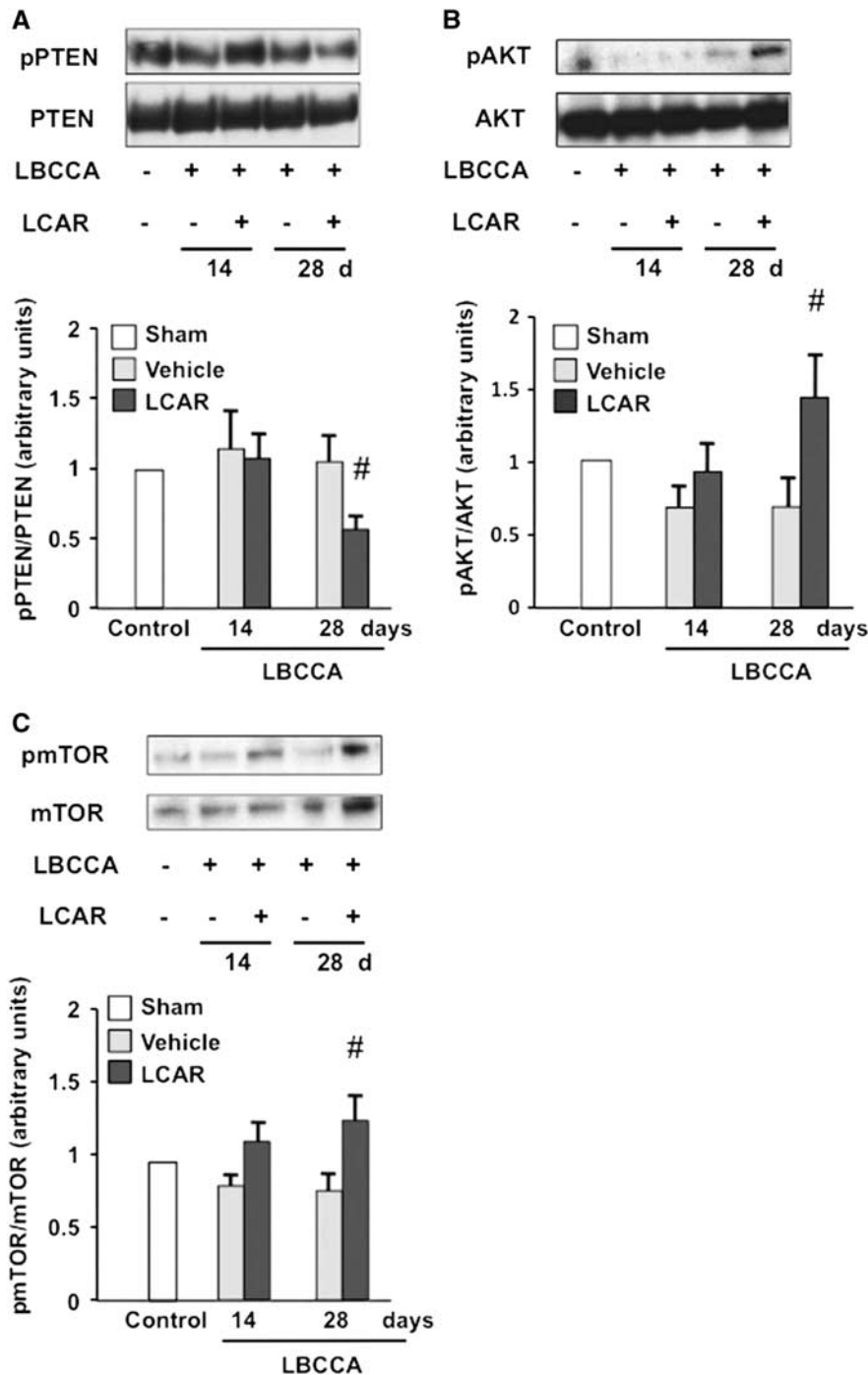


**Figure 3.** L-carnitine regulates phosphorylation of PTEN, AKT, and mTOR in the corpus callosum of chronic hypoperfusion rats. (A–C) Western blot data showing phosphorylated phosphatase and tensin homolog deleted on chromosome 10 (PTEN, Ser 380/Thr 382/383, **A**), phosphorylated Akt (Ser 473, **B**), and phosphorylated mammalian target of rapamycin (mTOR, Ser 2448, **C**). Total PTEN, Akt, and mTOR levels were used as internal controls.  $N = 5/\text{group}$ . Values are expressed as mean  $\pm$  s.e.  $^{\#}p < 0.05$  versus the vehicle-treated rats.

immediately after LBCCA and lasting 2 to 3 days, CBF is substantially reduced and remains very low, which creates hypoxic and ischemic conditions in white matter. The chronic phase lasts 8 to 12 weeks after the acute phase and is characterized by compensatory increases in CBF *via* collateral vessels.<sup>5</sup> During the chronic phase, inflammatory changes, oxidative stress, and astrogliosis are induced in white matter, and the degree of histologic change in WMLs is consistent with the decreases in CBF.<sup>25</sup> The

current data showed that continuous treatment with L-carnitine did not affect CBF but improved WMLs. Thus, it is suggested that L-carnitine exerted direct neuroprotective effects against LBCCA injury.

Stroke induces an acute loss of pNFH<sup>+</sup> axons in mammalian brains.<sup>26</sup> Previously, it was reported that pNFH<sup>+</sup> axons were increased in the peri-infarct cortex during stroke recovery in a rat model of permanent middle cerebral artery occlusion, and that

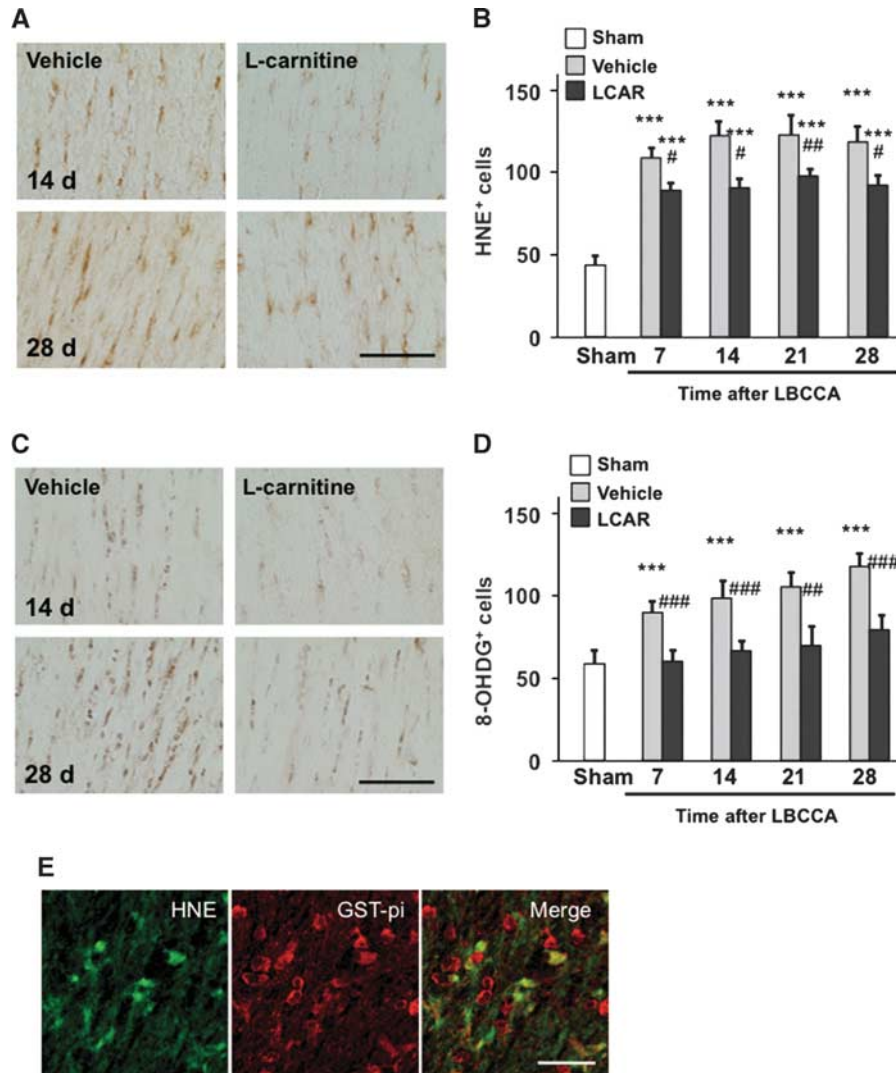


**Figure 4.** carnitine reduces oxidative stress in oligodendrocytes after chronic hypoperfusion. **(A)** Representative images of 4-hydroxy-2-nonenal (HNE) immunostaining show the accumulation of lipid peroxidation in oligodendrocytes at 14 and 28 days post ligation of the bilateral common carotid arteries (LBCCA) in vehicle-treated and L-carnitine (LCAR)-treated rats. **(B)** Quantitation of HNE<sup>+</sup> cell numbers in the corpus callosum. **(C)** Representative images of 8-hydroxy-deoxyguanosine (8OHdG) immunostaining show oxidative DNA damage in oligodendrocytes at 14 and 28 days in vehicle-treated and L-carnitine-treated rats. **(D)** Quantitation of 8OHdG<sup>+</sup> cell numbers in the corpus callosum. Values are expressed as mean  $\pm$  s.e.  $N = 4$ /group. Bars = 40  $\mu$ m. \*\*\* $P < 0.001$  versus the sham-operated group, and # $P < 0.05$ , ## $P < 0.01$ , and ### $P < 0.001$  versus the vehicle-treated group. **(E)** Double immunofluorescent confocal images of representative vehicle-treated rats at 28 days post LBCCA showing HNE<sup>+</sup> cells colocalized with glutathione-S-transferase-pi (GST-pi)<sup>+</sup> oligodendrocytes. Bars = 20  $\mu$ m.

PTEN/Akt/glycogen synthase kinase-3 $\beta$  signaling promoted axonal outgrowth in cultured cortical neurons after ischemia.<sup>18</sup> In cultured cortical neurons, a local reduction of PTEN and activation of mTOR by miR-17-92 cluster in distal axons enhanced axonal outgrowth.<sup>27</sup> Others have shown that deleting PTEN enhances regeneration of axons in adult corticospinal neurons after spinal cord injury.<sup>28</sup> The PTEN inhibits phosphoinositide 3-kinase/Akt signaling.<sup>29</sup> Activation of Akt and subsequent phosphorylation of mTOR increases axonal outgrowth.<sup>30</sup> In the current study, L-carnitine increased pNFH during the chronic stage of LBCCA injury, which was associated with downregulation of PTEN and activation of Akt and mTOR. Additionally, phosphorylated Akt and mTOR were expressed in pNFH<sup>+</sup> axons. Thus, this is the first report to show that L-carnitine enhances pNFH in response to regulation of the PTEN/Akt/mTOR signaling pathway in the corpus callosum of the rat chronic hypoperfusion model.

Loss of oligodendrocytes and demyelination are pathologic hallmarks of ischemic white-matter disease, which is associated with vascular dementia.<sup>31</sup> HNE and 8OHdG proteins accumulate after ischemia.<sup>6,32</sup> MBP<sup>+</sup> processes in oligodendrocytes are acutely decreased after hypoxia-ischemia induced white-matter damage, whereas myelin sheath generation and axonal myelination are facilitated during the chronic recovery stage in ischemic rats.<sup>18,33</sup> Our data show that L-carnitine substantially suppresses the production of HNE and 8OHdG in oligodendrocytes after chronic hypoperfusion. Intriguingly, continuous treatment with L-carnitine increases MBP expression and axonal myelination from baseline levels. Although stroke mediates free radical formation and injures oligodendrocytes and axons, the current data suggest that L-carnitine not only exerts an antioxidant effect through the suppression of lipid peroxidation and oxidative DNA damage, but may also facilitate development and myelination of

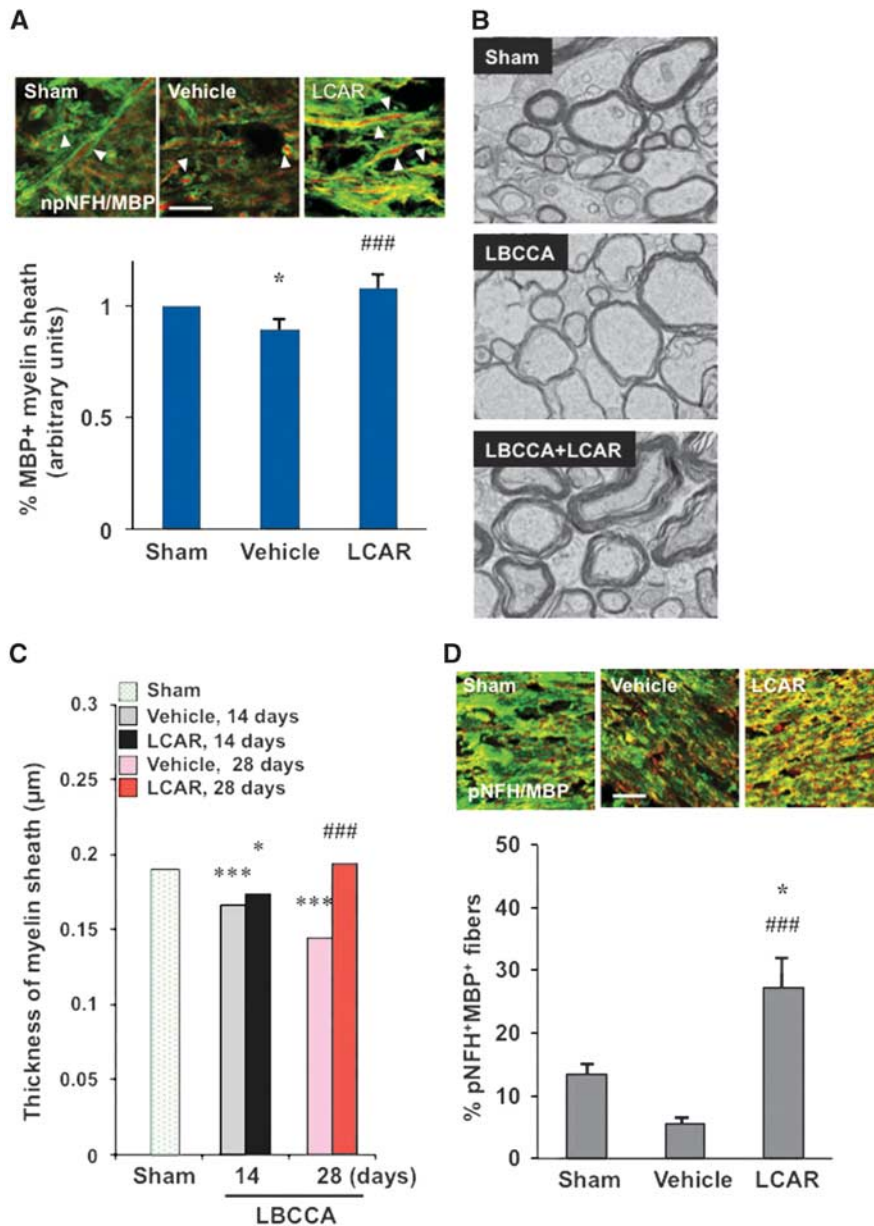


**Figure 5.** L-carnitine increases myelin sheath thickness after chronic hypoperfusion. **(A)** Double immunofluorescent confocal images of representative rats at 28 days post ligation of the bilateral common carotid arteries (LBCCA) from sham-operated, vehicle-treated, and L-carnitine (LCAR)-treated animals, showing nonphosphorylated high molecular weight neurofilament (npNFH)<sup>+</sup> fibers surrounded by myelin basic protein (MBP)<sup>+</sup> processes (arrowheads). Bar = 10 μm. Quantitation of the diameter of MBP<sup>+</sup> processes in the corpus callosum. *N* = 4/group. **(B)** Representative electron microscopic images at 28 days after LBCCA in sham-operated, vehicle-treated, and L-carnitine-treated rats, showing axons of unequal size surrounded by myelin sheaths. Bar = 1 μm. **(C)** Quantitation of average myelin sheath thickness in sham-operated animals, and at 14 and 28 days after LBCCA in vehicle-treated and LCAR-treated rats. *N* = 4/group. **(D)** Double immunofluorescent confocal images of representative rats at 28 days post LBCCA from sham-operated, vehicle-treated, LCAR-treated animals, showing phosphorylated high molecular weight neurofilament (pNFH)<sup>+</sup> and MBP<sup>+</sup> fibers. Bar = 20 μm. Quantitation of pNFH<sup>+</sup> axons colocalized with MBP<sup>+</sup> processes in the corpus callosum. *N* = 4/group. Values are expressed as mean ± s.e. \**P* < 0.05, \*\*\**P* < 0.001 versus the sham-operated group, and ###*P* < 0.001 versus the vehicle-treated group.

oligodendrocytes in the corpus callosum after chronic cerebral hypoperfusion.

Mitochondrial dysfunction is essential in the pathophysiology of diverse neurologic diseases, including stroke.<sup>34,35</sup> Because reactive oxygen species are mainly generated as byproducts of mitochondrial respiration, mitochondria are thought to be the primary target of oxidative damage.<sup>36</sup> L-carnitine functions in the mitochondria in the transport of long-chain fatty acids into the mitochondrial matrix and facilitates β-oxidation.<sup>37</sup> L-carnitine

prevented the reduction of CPT1 and CPT2 after oxygen-glucose deprivation in cultured hippocampal slices.<sup>38</sup> CPT1C regulates dendritic spine maturation and is related to cognitive function in mice.<sup>39</sup> Our data have shown that continuous treatment with L-carnitine ameliorates mitochondrial inner and outer membrane dysfunction after chronic hypoperfusion. The present study is the first to show that impairment of mitochondrial membrane function is implicated as an essential mechanism of WMLs induced by chronic hypoperfusion, and that L-carnitine improves

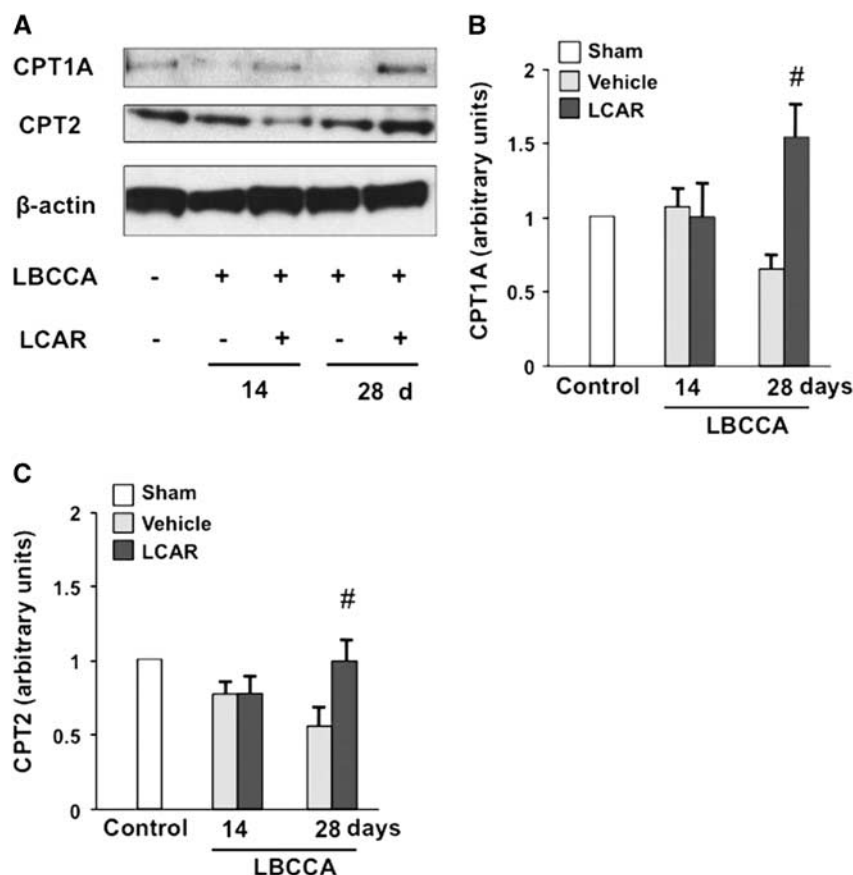


**Figure 6.** L-carnitine improves carnitine palmitoyltransferase levels after chronic hypoperfusion. (A–C) Carnitine palmitoyltransferase 1A (CPT1A) and CPT2 levels measured using western blots.  $\beta$ -Actin was used as an internal control.  $N = 5/\text{group}$ . Values are expressed as mean  $\pm$  s.e. <sup>#</sup> $P < 0.05$  versus vehicle-treated rats. LBCCA, ligation of the bilateral common carotid arteries; LCAR, L-carnitine.

mitochondrial membrane dysfunction, thereby lessening oxidative stress and enhancing axonal plasticity and myelination.

In conclusion, axonal impairment is critically implicated in WMLs induced by chronic cerebral hypoperfusion. The molecular mechanisms underlying axonal plasticity and mitochondrial dysfunction associated with WMLs have previously been unknown. The current study provides evidence that L-carnitine improves mitochondrial membrane dysfunction and alleviates oxidative stress, thereby enhancing axonal plasticity and oligodendrocytic axonal myelination, which is likely to form the basis of the neuroprotective effects of L-carnitine against WMLs and cognitive impairment.

#### DISCLOSURE/CONFLICT OF INTEREST

The authors declare no conflict of interest.

#### ACKNOWLEDGMENTS

The authors thank Reiko Ishikawa for providing technical assistance.

#### REFERENCES

- Zhang K, Sejnowski TJ. A universal scaling law between gray matter and white matter of cerebral cortex. *Proc Natl Acad Sci USA* 2000; **97**: 5621–5626.
- Vermeer SE, Prins ND, den Heijer T, Hofman A, Koudstaal PJ, Breteler MM. Silent brain infarcts and the risk of dementia and cognitive decline. *N Engl J Med* 2003; **348**: 1215–1222.
- Dewar D, Underhill SM, Goldberg MP. Oligodendrocytes and ischemic brain injury. *J Cereb Blood Flow Metab* 2003; **23**: 2632–2674.
- Terasaki Y, Liu Y, Hayakawa K, Pham LD, Lo EH, Ji X *et al*. Mechanisms of neurovascular dysfunction in acute ischemic brain. *Curr Med Chem* 2014; **21**: 2035–2042.

- Farkas E, Luiten PG, Bari F. Permanent, bilateral common carotid artery occlusion in the rat: a model for chronic cerebral hypoperfusion-related neurodegenerative diseases. *Brain Res Rev* 2007; **54**: 162–180.
- Ueno Y, Zhang N, Miyamoto N, Tanaka R, Hattori N, Urabe T. Edaravone attenuates white matter lesions through endothelial protection in a rat chronic hypoperfusion model. *Neuroscience* 2009; **162**: 317–327.
- Watanabe T, Zhang N, Liu M, Tanaka R, Mizuno Y, Urabe T. Cilostazol protects against brain white matter damage and cognitive impairment in a rat model of chronic cerebral hypoperfusion. *Stroke* 2006; **37**: 1539–1545.
- Roe CR, Bohan TP. L-carnitine therapy in propionicacidemia. *Lancet* 1982; **1**: 1411–1412.
- Ringseis R, Keller J, Eder K. Mechanisms underlying the anti-wasting effect of L-carnitine supplementation under pathologic conditions: Evidence from experimental and clinical studies. *Eur J Nutr* 2013; **52**: 1421–1442.
- Iliceto S, Scrutinio D, Bruzzi P, D'Ambrosio G, Boni L, Di Biase M *et al*. Effects of L-carnitine administration on left ventricular remodeling after acute anterior myocardial infarction: the L-Carnitine Ecocardiografia Digitalizzata Infarto Miocardico (CEDIM) Trial. *J Am Coll Cardiol* 1995; **26**: 380–387.
- Delaney CL, Spark JI, Thomas J, Wong YT, Chan LT, Miller MD. A systematic review to evaluate the effectiveness of carnitine supplementation in improving walking performance among individuals with intermittent claudication. *Atherosclerosis* 2013; **229**: 1–9.
- Stanley WC, Lopaschuk GD, Hall JL, McCormack JG. Regulation of myocardial carbohydrate metabolism under normal and ischaemic conditions. Potential for pharmacological interventions. *Cardiovasc Res* 1997; **33**: 243–257.
- Al-Majed AA, Sayed-Ahmed MM, Al-Omar FA, Al-Yahya AA, Aleisa AM, Al-Shabanah OA. Carnitine esters prevent oxidative stress damage and energy depletion following transient forebrain ischaemia in the rat hippocampus. *Clin Exp Pharmacol Physiol* 2006; **33**: 725–733.
- Lolic MM, Fiskum G, Rosenthal RE. Neuroprotective effects of acetyl-L-carnitine after stroke in rats. *Ann Emerg Med* 1997; **29**: 758–765.
- Rosenthal RE, Williams R, Bogaert YE, Getson PR, Fiskum G. Prevention of post-ischemic canine neurological injury through potentiation of brain energy metabolism by acetyl-L-carnitine. *Stroke* 1992; **23**: 1312–1317.

- 16 Li S, Overman JJ, Katsman D, Kozlov SV, Donnelly CJ, Twiss JL *et al*. An age-related sprouting transcriptome provides molecular control of axonal sprouting after stroke. *Nat Neurosci* 2010; **13**: 1496–1504.
- 17 Liu Z, Li Y, Zhang ZG, Cui X, Cui Y, Lu M *et al*. Bone marrow stromal cells enhance inter- and intracortical axonal connections after ischemic stroke in adult rats. *J Cereb Blood Flow Metab* 2010; **30**: 1288–1295.
- 18 Ueno Y, Chopp M, Zhang L, Buller B, Liu Z, Lehman NL *et al*. Axonal outgrowth and dendritic plasticity in the cortical peri-infarct area after experimental stroke. *Stroke* 2012; **43**: 2221–2228.
- 19 Andreozzi GM, Martini R, Cordova RM, D'Eri A. L-propionyl-carnitine protects tissues from ischaemic injury in an 'in vivo' human ischaemia-reperfusion model. *Clin Drug Investig* 2002; **22**: 15–21.
- 20 Harada H, Wang Y, Mishima Y, Uehara N, Makaya T, Kano T. A novel method of detecting rCBF with laser-Doppler flowmetry without cranial window through the skull for a MCAO rat model. *Brain Res Brain Res Protoc* 2005; **14**: 165–170.
- 21 Lescuyer P, Strub JM, Luche S, Diemer H, Martinez P, Van Dorsselaer A *et al*. Progress in the definition of a reference human mitochondrial proteome. *Proteomics* 2003; **3**: 157–167.
- 22 Ek CJ, Habgood MD, Dennis R, Dziegielewska KM, Mallard C, Wheaton B *et al*. Pathological changes in the white matter after spinal contusion injury in the rat. *PLoS ONE* 2012; **7**: e43484.
- 23 de Waegh SM, Lee VM, Brady ST. Local modulation of neurofilament phosphorylation, axonal caliber, and slow axonal transport by myelinating Schwann cells. *Cell* 1992; **68**: 451–463.
- 24 Sánchez I, Hassinger L, Sihag RK, Cleveland DW, Mohan P, Nixon RA. Local control of neurofilament accumulation during radial growth of myelinating axons in vivo. Selective role of site-specific phosphorylation. *J Cell Biol* 2000; **151**: 1013–1024.
- 25 Miki K, Ishibashi S, Sun L, Xu H, Ohashi W, Kuroiwa T *et al*. Intensity of chronic cerebral hypoperfusion determines white/gray matter injury and cognitive/motor dysfunction in mice. *J Neurosci Res* 2009; **87**: 1270–1281.
- 26 Bidmon HJ, Jancsik V, Schleicher A, Hagemann G, Witte OW, Woodhams P *et al*. Structural alterations and changes in cytoskeletal proteins and proteoglycans after focal cortical ischemia. *Neuroscience* 1998; **82**: 397–420.
- 27 Zhang Y, Ueno Y, Liu XS, Buller B, Wang X, Chopp M *et al*. The MicroRNA-17-92 cluster enhances axonal outgrowth in embryonic cortical neurons. *J Neurosci* 2013; **33**: 6885–6894.
- 28 Liu K, Lu Y, Lee JK, Samara R, Willenberg R, Sears-Kraxberger I *et al*. PTEN deletion enhances the regenerative ability of adult corticospinal neurons. *Nat Neurosci* 2010; **13**: 1075–1081.
- 29 Jiang H, Guo W, Liang X, Rao Y. Both the establishment and the maintenance of neuronal polarity require active mechanisms: Critical roles of GSK-3beta and its upstream regulators. *Cell* 2005; **120**: 123–135.
- 30 Christie KJ, Webber CA, Martinez JA, Singh B, Zochodne DW. PTEN inhibition to facilitate intrinsic regenerative outgrowth of adult peripheral axons. *J Neurosci* 2010; **30**: 9306–9315.
- 31 Jellinger KA. The enigma of vascular cognitive disorder and vascular dementia. *Acta Neuropathol* 2007; **113**: 349–388.
- 32 McCracken E, Valeriani V, Simpson C, Jover T, McCulloch J, Dewar D. The lipid peroxidation by-product 4-hydroxynonenal is toxic to axons and oligodendrocytes. *J Cereb Blood Flow Metab* 2000; **20**: 1529–1536.
- 33 Manning SM, Talos DM, Zhou C, Selip DB, Park HK, Park CJ *et al*. NMDA receptor blockade with memantine attenuates white matter injury in a rat model of periventricular leukomalacia. *J Neurosci* 2008; **28**: 6670–6678.
- 34 Lin MT, Beal MF. Mitochondrial dysfunction and oxidative stress in neurodegenerative diseases. *Nature* 2006; **443**: 787–795.
- 35 Niizuma K, Endo H, Chan PH. Oxidative stress and mitochondrial dysfunction as determinants of ischemic neuronal death and survival. *J Neurochem* 2009; **109** (Suppl 1): 133–138.
- 36 Wang T, Gu J, Wu PF, Wang F, Xiong Z, Yang YJ *et al*. Protection by tetrahydroxystilbene glucoside against cerebral ischemia: Involvement of JNK, SIRT1, and NF-kappaB pathways and inhibition of intracellular ROS/RNS generation. *Free Radic Biol Med* 2009; **47**: 229–240.
- 37 Scholte HR, Stinis JT, Jennekens FG. Low carnitine levels in serum of pregnant women. *N Engl J Med* 1978; **299**: 1079–1080.
- 38 Rau TF, Lu Q, Sharma S, Sun X, Leary G, Beckman ML *et al*. Oxygen glucose deprivation in rat hippocampal slice cultures results in alterations in carnitine homeostasis and mitochondrial dysfunction. *PLoS ONE* 2012; **7**: e40881.
- 39 Carrasco P, Sahún I, McDonald J, Ramírez S, Jacas J, Gratacós E *et al*. Ceramide levels regulated by carnitine palmitoyltransferase 1C control dendritic spine maturation and cognition. *J Biol Chem* 2012; **287**: 21224–21232.